New Phytologist

Tree ring ^{14}C and ^{13}C content reveal reliance on fast cycling carbon for pine growth in semiarid montane forests

Steven A. Kannenberg[1,2]*, William E. Wright[3]*, James R. Ehleringer[2] and Russell K. Monson[3,4,5]

[1]Department of Biology, West Virginia University, Morgantown, WV 26505, USA; [2]School of Biological Sciences, University of Utah, Salt Lake City, UT 84112, USA; [3]Laboratory of Tree Ring Research, University of Arizona, Tucson, AZ 85721, USA; [4]Department of Ecology and Evolutionary Biology, University of Arizona, Tucson, AZ 85721, USA; [5]Department of Ecology and Evolutionary Biology, University of Colorado, Boulder, CO 80309, USA

Author for correspondence:
Steven A. Kannenberg
Email: steven.kannenberg@mail.wvu.edu

Received: *14 June 2025*
Accepted: *13 August 2025*

New Phytologist (2025) **248:** 1728–1739
doi: 10.1111/nph.70539

Key words: carbon reserves, dendrochronology, drought, isotope fractionation, *Pinus ponderosa*, radiocarbon, vapor pressure deficit.

Summary

- Trees harbor large stores of nonstructural carbohydrates, some of which are quite old (> 10 yr), yet we know little of how these older stores may be used for woody growth. Crucially, the use of old carbohydrates during cellulose biosynthesis could confound climate reconstructions that rely on tree ring stable isotope ratios.
- We analyzed tree-ring cellulose $\Delta^{14}C$ and $\delta^{13}C$ in earlywood of two pine species from montane forests in western North America using tree rings produced during the radiocarbon bomb pulse (1966–1980).
- Comparison of the $\Delta^{14}C$ from ponderosa pine in Utah with estimates of atmospheric $^{14}CO_2$ showed that the cellulose $\Delta^{14}C$ values can be explained using only carbon fixed in the same growing season as ring construction. In the more arid Arizona pine, the cellulose $\Delta^{14}C$ values indicate that up to 50% of the carbon used in tree-ring construction can be from photosynthate assimilated the year before ring construction. Correlations between cellulose $\delta^{13}C$ time series and aridity indices validated the results obtained from $\Delta^{14}C$ values.
- The results reveal that in some semiarid coniferous forests, tree-ring isotope composition could partially reflect the climate from at least one previous growing season, but that carbon sources older than 2 yr are likely seldom used.

Introduction

Analyses of the stable isotope ratios of carbon and oxygen from tree ring cellulose have been used for decades to reconstruct the growth responses of trees to environmental variation (e.g. Gessler *et al.*, 2013; Leavitt & Roden, 2022). One of the underlying assumptions of tree ring stable isotope reconstructions is that observed isotopic ratios can be explained by fractionation models driven by the climate and atmospheric conditions that existed during the same year that each ring was formed. This assumption has been challenged by some studies showing that pools of older carbon and newly assimilated carbon coexist in stemwood tissues (Richardson *et al.*, 2013, 2015) and may sometimes be radially mixed with younger carbon pools (Richardson *et al.*, 2015; Hartmann & Trumbore, 2016). Such evidence that both old and new carbon is available and may be mixed in woody tissues brings up questions as to whether we can rely on our past assumptions about tree ring isotope reconstructions.

Carbon-based stores in plants occur in the form of nonstructural carbohydrates (NSCs), mostly sugars and starch. The storage of vital resources is an important evolutionary hedge against times when they are not available and is part of the survival strategy of both plants and animals. When phenological needs or environmental stressors cause a critical process within a plant to require more NSCs than are immediately available through photosynthesis, then either stored NSCs will be mobilized (e.g. Hoch *et al.*, 2003; Kuptz *et al.*, 2011; Richardson *et al.*, 2013; Dobbelstein *et al.*, 2018; Furze *et al.*, 2018), or the critical process (e.g. primary cell wall expansion, secondary cell wall deposition) will be passively or actively downregulated (e.g. Dietze *et al.*, 2014; de Dios & Gessler, 2021; Huang *et al.*, 2021). Results of recent modeling and empirical research indicate that NSCs in the woody tissues of plants are best modeled using two pools: a younger fast-turnover pool and an older slow-turnover pool (Carbone *et al.*, 2013; Richardson *et al.*, 2013, 2015; Hartmann & Trumbore, 2016; McCarroll *et al.*, 2017). The slower pool has been shown to persist for several years to more than a decade (Richardson *et al.*, 2013).

There is uncertainty about the degree to which woody stem growth draws upon the slow turnover pools. Evidence that the faster pool is used to support radial stem growth has been reported for various deciduous angiosperms and deciduous conifers through the use of radiocarbon analysis (Carbone *et al.*, 2013), stable isotope labeling (Kagawa *et al.*, 2006a,b), and statistical relationships between stable isotope ratios in consecutive tree rings (e.g. Switsur *et al.*, 1995; Richardson *et al.*, 2013; Kimak & Leuenberger, 2015;

*These authors contributed equally to this work.

McCarroll *et al*., 2017). The case for evergreen conifers is less certain. While there is ample evidence of the presence of new and old NSCs in evergreen wood (e.g. Richardson *et al*., 2015), direct evidence for the incorporation of stored carbon into the stem growth of evergreen conifers has only been reported from observations using stable isotope pulse labeling in *Podocarpus* growing in a subhumid tropical forest in Ethiopia (Krepkowsi *et al*., 2013), in an elevated CO_2 study of *Picea* growing in a temperate site in Switzerland (Mildner *et al*., 2015), and statistical analyses of stable carbon isotope time series from the wood in two Chinese pine species (Fu *et al*., 2017). However, in these cases the ages of the stored carbon sources that were used during growth were unresolved. By contrast, some evidence exists that evergreen conifers largely rely on newly fixed carbon for radial growth (e.g. Rinne-Garmston *et al*., 2023). Thus, the age of carbon used for coniferous tree growth is not well quantified, and the potential for carbon source mixing to affect assumptions about tree–climate interactions in dendrochronological studies is an open issue.

To further investigate the use of carbon stores in evergreen conifers, we determined the radiocarbon content of the first half of earlywood (EW) cellulose isolated from two members of the ponderosa pine species complex (e.g. Willyard *et al*., 2016; Supporting Information Notes S1), *Pinus arizonica* and *Pinus ponderosa* variant *brachyptera*. Trees in two mountain ranges were studied: a relatively dry montane site in the Santa Catalina Mountains near Tucson, Arizona, and a more mesic site in the Wasatch Mountains near Salt Lake City, Utah. We tested three alternative hypotheses: (1) that a significant amount of 'old', slow-cycling carbon, which was assimilated in distant prior years (> 2 yr), is present in the first half of EW of the annual rings; (2) that a significant amount of 'new', fast-cycling carbon assimilated in recent years (≤ 2 yr) is present in the first half of EW of the annual rings; and (3) that only carbon assimilated during the current growing season was used to form the first half of EW of the annual rings. By choosing sites for pines in two different montane climate zones, we also tested the hypothesis that growth in the face of more frequent water stress causes an increased reliance on stored carbon as either 'new', fast-cycling carbon or 'old', slow-cycling carbon.

Materials and Methods

General approach

Our overall approach was predicated on the theory that the use of older carbon during the years following aboveground nuclear testing is quantitatively revealed as deviations in ^{14}C content ($\Delta^{14}C$) in tree rings from that of atmospheric $^{14}CO_2$ that is assimilated during the same year as ring formation. Zonal time series of atmospheric $^{14}CO_2$ provide expected values for the ^{14}C fixed during photosynthesis, assuming contributions from respired or nonbiological ^{14}C are negligible. Cellulose ^{14}C values that match these expectations would support an understanding that the cellulose was synthesized from NSCs produced during the current growing season, while offsets from the expected values would be evidence for the incorporation of NSCs produced and stored before the current growing season.

Details of study sites

The Arizona *Pinus* site (32.4°N, 110.7°W), populated by *Pinus arizonica* Engelm., is characterized as a 'semiarid' exposed climate at 2330 m elevation on a southwestern aspect. Mean annual temperature is 12.4°C and average annual precipitation is *c*. 800 mm, with *c*. 40% falling during the summer. The Utah *Pinus ponderosa* Douglas ex C. Lawson site is in Big Cottonwood Canyon (40.6°N, 111.6°W) in the Wasatch Mountains of northeastern Utah. Samples were collected at the base of an exposed southern-aspect slope from trees of the same approximate age as those of the Arizona trees. The mean annual precipitation at the site averages *c*. 1000 mm, and the mean annual temperature is 3.9°C (PRISM 1981–2010; Daly *et al*., 2008). About 90% of the annual precipitation falls as snow between November and April, with the remaining 10% occurring as convective rain between July and September. Both sites have an open canopy stand structure, allowing for rapid removal of sub-canopy CO_2 from soil respiration and sub-canopy vegetation, and they are high elevation sites removed from vehicle exhaust near roadways. See Notes S1 for more details on the study sites. The annual tree-ring chronology in trees from both sites is clearly distinguishable at a coarse anatomical level as EW (produced during spring and early summer) and latewood (produced during mid-to-late summer; Notes S2; Figs S1, S2). We focused our observations on the spring growth in the annual tree rings because these are the portions of the ring most sensitive to interannual dynamics in winter precipitation (Sheppard *et al*., 2002; Szejner *et al*., 2016).

Sample collection and preparation

Samples (n = 20–25 trees) from the Arizona and Utah tree sites were collected using a 12-mm increment borer, from which the average tree age across both sites was determined to be *c*. 80 yr. The annual ring patterns on each core were compared visually and digitally to confirm crossdating. After crossdating, a subset of the trees (n = 4–5 trees) was selected from each site for further processing and isotope analysis. A general summary of the steps between subset selection and isotope analysis was as follows: (1) tree rings between 1966 and 1980 were identified; (2) the first half of the EW (Utah) or the EW formed before the intraannual density fluctuations (Arizona) (see Notes S2 for more explanation), both labeled EW, were subdivided from each core and separately labeled and stored; (3) each EW subdivision was ground to 20 mesh (*c*. 840 μm); (4) ground samples were sealed in separate pouches using a permeable pouching material; (5) α-cellulose was extracted from the ground samples using a modified Jayme–Wise method; (6) the α-cellulose was further homogenized using probe sonication. Details about these steps are available in Methods S1. Our intention in using the initial portion of the EW was to capture the period where we would most likely expect the use of carbon stored from before the current growing season; we would expect latewood isotopic signatures to be much more supported by current year photosynthesis.

Atmospheric ^{14}C and annual plant sample collection

Due to unique atmospheric mixing patterns, the $^{14}CO_2$ content of the atmosphere varies geographically and interannually. Time series of estimated global atmospheric $^{14}CO_2$ content divides the globe into zonal bands of similar atmospheric $^{14}CO_2$. Zone 1 and Zone 2 in the northern hemisphere divide the United States at the downwelling point between large-scale atmospheric circulation cells, the Hadley Cell and the Ferrel Cell, placing Tucson, Arizona, *c.* 32°N, in Zone 2 and Salt Lake City, Utah, *c.* 41°N, at the transition between Zone 1 and Zone 2 (Hua *et al.*, 2022). The datasets used to construct the $^{14}CO_2$ time series from Hua *et al.* (2022) are based on both direct atmospheric measurements and tree-ring proxies. While the number of stations and chronologies is fairly small (< 20 per zone), atmospheric mixing is rapid, and the station locations were away from other sources of radiocarbon, which should result in a clean isotopic signal.

To accomplish a local validation of the zonal designations provided by Hua *et al.* (2022), we assembled an additional set of ^{14}C analyses using dried tissue from annual plants collected near the study sites and archived in regional herbaria. We only sampled annual plant specimens collected at higher elevations and/or laterally removed from any nearby cities and major roadways. The Arizona annual plants were collected 22 ± 18.4 miles away (mean ± SD) from the tree-ring samples, while the Utah annual plants were collected 39.4 ± 16.8 miles away. Additional details about the acquisition and sampling of the annual plant specimens are available in Notes S3. The species, their metadata including specific collection locations, and the resulting radiocarbon values are also provided (Table S1).

Stable isotope measurements and analysis

To further quantify how current/previous year climate may have influenced carbon dynamics, we assessed the correlation between $\delta^{13}C$ and aridity indexes using EW α-cellulose $\delta^{13}C$ time series from the two pine species – Arizona pine from Arizona (1966–2014) and ponderosa pine from Utah (1971–2020). The time series for Arizona pine was spliced together from two different sources – one from 1985 to 2014 (Belmecheri *et al.*, 2018; n = 30 yr, minus 2000 and 2002 because an EW division was not isolated for those years) and one from 1966 to 1980 (n = 15 yr; from this study). Both data sources were from the same Santa Catalina Mountain study site, and the significance of correlation coefficients when the time series were plotted separately was very similar; thus, we combined them (Notes S4). The $\delta^{13}C$ time series used for ponderosa pine (n = 50 yr) in Utah was constructed as part of this study.

Generally, $^{13}C/^{12}C$ ratios ($\delta^{13}C$) were measured from the CO_2 produced during α-cellulose combustion using an elemental analyzer isotope ratio mass spectrometer (EA-IRMS). Samples used from the Belmecheri *et al.* (2018) study were measured at the University of Maryland Stable Isotope Laboratory. The samples collected for this study were measured at the Stable Isotope Ratio Facility of Environmental Research (SIRFER) at the University of Utah using a Thermo Finnigan Delta Plus XL EA-IRMS, as described previously in Fiorella *et al.* (2022). The overall precision for $\delta^{13}C$ values used in the time series was 0.1‰. Corrections to the isotope measurements were made to account for changes in the atmospheric $^{13}C/^{12}C$ ratio due to past-century fossil fuel combustion (Suess, 1955) and for the influence of progressive increases in atmospheric CO_2 on direct and indirect changes in the intercellular to ambient CO_2 concentration (c_i/c_a) (McCarroll *et al.*, 2008). The latter correction, often called the 'PIN' correction, is less commonly applied, though it did not affect our conclusions. The 'PIN' correction ended up slightly increasing our correlation coefficients between vapor pressure deficit (VPD) and $\delta^{13}C$ in general, though across all sites and months, the greatest change in correlation coefficient was 0.07; therefore, we decided on its inclusion.

We focused on mean monthly atmospheric VPD and SPEI (standard precipitation evapotranspiration index) as the principal determinant of dynamics in $\delta^{13}C$. We justify this decision as follows: (1) atmospheric aridity limits surface conductance and evapotranspiration more than soil moisture in many temperate latitude forests (Novick *et al.*, 2016; Ficklin & Novick, 2017), and (2) atmospheric aridity has been identified as the factor most correlated with drought-associated declines in global gross primary productivity during the past 20 yr (Yuan *et al.*, 2019). Datasets of VPD were produced for each tree site using data available from the PRISM website (https://prism.oregonstate.edu/explorer/), with downloads specified for 4 km^2 grid cells that included the location of each tree site. For SPEI analyses, we used 5 km^2 data from NOAA (https://www.drought.gov/data-maps-tools/us-gridded-standardized-precipitation-index-spei-nclimgrid-monthly), again specified for the grid cells that included the location of each tree site.

Radiocarbon analysis

Graphitization and radiocarbon analysis were done in the Keck Radiocarbon Laboratory, UC Irvine, Irvine, California (Beverly *et al.*, 2010). Calibration was done using cellulose standards, IAEA-C3 and FIRI-G. Background subtractions were done using ^{14}C-free wood dated to the Pliocene. The average precision of the $\Delta^{14}C$ analyses was 2.2‰. In order to quantify the role of previously assimilated carbon for radial growth, we modeled $\Delta^{14}C$ under five scenarios, whereby 0, 25, 50, 75, and 100% of the carbon used to construct wood was derived from the previous year's atmospheric $\Delta^{14}C$. See Methods S1 for details regarding sample extraction and processing. Additionally, see Notes S5 for a discussion on errors in $\Delta^{14}C$ and $\delta^{13}C$ data, which are very low relative to the magnitude of their values.

Results

Atmospheric $\Delta^{14}CO_2$ and $\Delta^{14}C$ from annual plants

A comparison of $\Delta^{14}C$ values from annual plant specimens collected near the Arizona and Utah sites is plotted in Fig. 1 against the Zone 1 and Zone 2 atmospheric $\Delta^{14}CO_2$ time series (all $R^2 > 0.99$, $P < 0.0001$). The atmospheric $\Delta^{14}CO_2$ time series

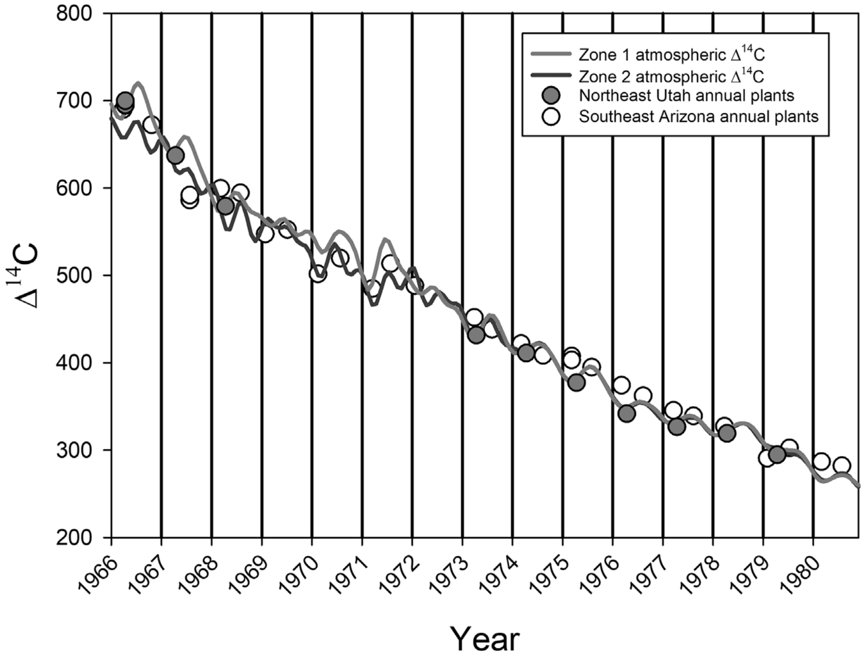

Fig. 1 Annual plant ^{14}C content plotted against Zone 1 and Zone 2 atmospheric $\Delta^{14}CO_2$. Zone 1 and Zone 2 atmospheric $\Delta^{14}CO_2$ are plotted as 3-month running averages based on 1-month estimates from Hua *et al*. (2022). Annual plant ^{14}C content is plotted for Arizona and Utah specimens. Overlapping white circles in the third quarter of 1967 and the first quarter of 1975 represent multiple analyses from the same specimen. Values for Zones 1 and 2 as estimated by Hua *et al*. (2022) are equal after 1973, so plots of the Zone 1 and Zone 2 time series after 1973 are identical.

are plotted as 3-month running averages, with the annual plant Δ^{14}C values plotted 30 d before their respective collection dates as an estimate of the timing of carbon input to the annual plants. A seasonal influence on the atmospheric $\Delta^{14}CO_2$ was obvious during the early years of the bomb pulse, with values decreasing slightly during winter and increasing in summer. The sample values from the Arizona annual plants do not match the Zone 2 time series perfectly, but overall, annual plant cellulose Δ^{14}C from southeastern Arizona agreed with the time-dependent decline in atmosphere $\Delta^{14}CO_2$ in Zone 2 and matched the seasonal shifts (RMSE = 17.6). While Utah annual plant Δ^{14}C values aligned with both Zone 1 (RMSE = 5.4) and Zone 2 (RMSE = 19.6) atmospheric Δ^{14}C, it is clear that these specimens were more aligned with the Zone 1 radiocarbon time series.

Atmospheric $\Delta^{14}CO_2$ and Δ^{14}C from tree-ring α-cellulose

A comparison of Δ^{14}C results in Arizona pine against 3-month running means of atmospheric $\Delta^{14}CO_2$ for Zone 2 is shown in Fig. 2 (RMSE = 18.0). A 3-month mean was chosen to approximate the number of months required for maturation of the secondary cell walls in the EW subdivision (see Morino *et al.*, 2021). The α-cellulose Δ^{14}C values from the Arizona pine were plotted on the 15th day of June, which is the approximate midpoint of the time between the beginning and the end of cell wall thickening (maturation) for EW cells produced in the closely related ponderosa pine in the Santa Catalina Mountains (Morino *et al.*, 2021). Observed Δ^{14}C from the individually sampled trees exhibited similar values within each year, with interannual declines in concert with the zonal atmospheric $\Delta^{14}CO_2$. However, there were small deviations from the line for most of the years, with observed values generally being slightly above the atmospheric curve.

Standard anomalies of climate were calculated for each site for comparison with the α-cellulose Δ^{14}C values using a 60-yr baseline period (1961–2020). In the Arizona radiocarbon time series, 4 of the 15 yr analyzed (1966–1980) experienced weather with cool season droughts (winter precipitation < 1σ of the long-term time series mean), marked with black stars in Fig. 2, while 3 of the 15 yr experienced greater-than-normal cool season precipitation (winter precipitation > 1σ of the long-term time series mean), marked with white stars in Fig. 2. Standard anomalies of total precipitation and mean temperature for previous October–May and June–September for all 15 yr are available (Notes S6; Fig. S3). There were no statistically different offsets between observed cellulose Δ^{14}C values and atmospheric Δ^{14}C among years experiencing precipitation anomalies as compared with those in the normal range.

The Δ^{14}C results for ponderosa pine in Utah are plotted in Fig. 2 against means of atmospheric $\Delta^{14}CO_2$ in Zone 1 (RMSE = 8.6), Zone 2 (RMSE = 17.7), and the average of Zone 1 and Zone 2 (RMSE = 9.0). The Zone 2 and Zone 1/Zone 2 average time series are included because the tree site in northeastern Utah may be within the Zone 1/Zone 2 transition during some years, though this analysis also backs up our herbarium annual plant samples that show a better coherence with Zone 1 atmospheric $\Delta^{14}CO_2$. To account for the shorter growing season at higher latitudes when compared to the Arizona site, the observed Δ^{14}C values are plotted on June 30 in each year. Standardized anomalies for the Utah site indicate only 1 yr within the time series with winter precipitation < 1σ from the mean (Fig. 2, black star) and 2 yr with winter snowfall > 1σ from the mean (Fig. 2, white stars). Standard anomalies of total precipitation and mean temperature for previous October–May and June–September for all 15 yr are available (Notes S6; Fig. S4). For this site, once again, the relationship of the Δ^{14}C values of EW with

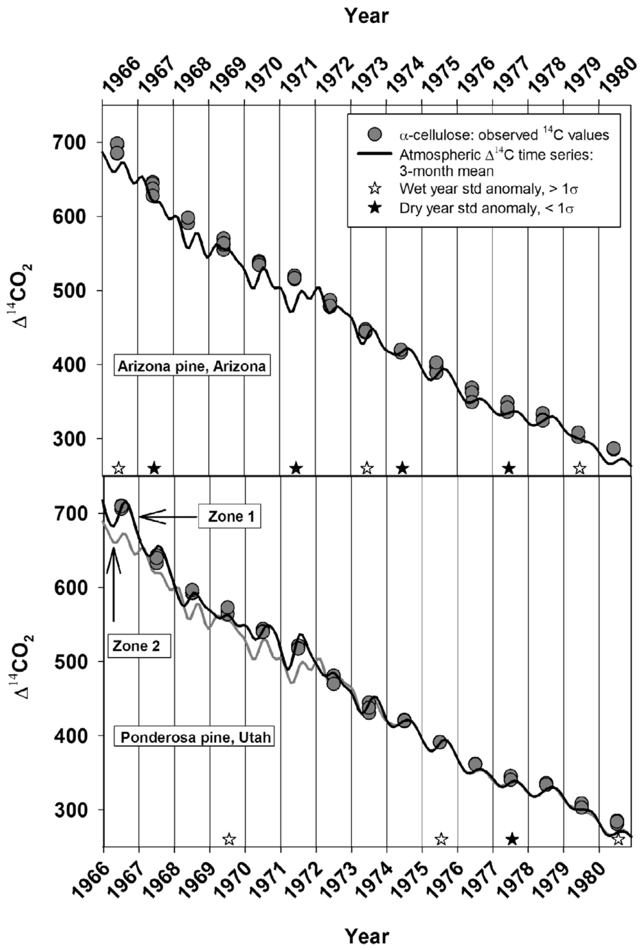

Fig. 2 Comparison of zonal estimates of atmospheric $\Delta^{14}C$ (Hua *et al*., 2022) as 3-month means and EW cellulose $\Delta^{14}C$ values for both study sites: Arizona pine, *Pinus arizonica* (n = 4) and Zone 2 atmospheric $\Delta^{14}C$, and Utah ponderosa pine, *Pinus ponderosa* (n = 3) and Zone 1 atmospheric $\Delta^{14}C$ (black line, indicated by horizontal arrow), Zone 2 atmospheric $\Delta^{14}C$ (gray line, indicated by vertical arrow). Standardized anomalies of precipitation exceeding $\pm 1\sigma$ as described in the main text for the mean of the previous November through the current June are indicated by white and black stars.

the zonal atmospheric $\Delta^{14}C$ values among the years experiencing precipitation anomalies was not different from those within the normal range; however, a possible cause of the larger positive offset for the 1980 cellulose ^{14}C value from the Zone 1 atmospheric $\Delta^{14}CO_2$ time series (Fig. 2) is presented using a subset of the 1979–1980 standard anomalies and SNOTEL data (Notes S7; Fig. S5).

Positive departures of $\Delta^{14}C$ values in tree-ring cellulose from the atmospheric $\Delta^{14}C$ present in the year of cellulose synthesis can primarily be explained by the incorporation of older NSCs stored in the tree. To analyze the potential for the use of stored carbon reserves, we produced five modeled time series of estimated cellulose $\Delta^{14}C$ depending on the differential use of NSCs (assumed to be reflective of atmospheric $\Delta^{14}C$) from the previous year: 0, 25, 50, 75, and 100%. These modeled curves are presented for both sites in Fig. 3, along with the mean of the $\Delta^{14}C$ cellulose values that were observed for each species. Comparisons of the observed EW cellulose $\Delta^{14}C$ values and these proportional atmospheric $\Delta^{14}C$ time series show that tree ring $\Delta^{14}C$ at the Arizona site is best explained by the model for 50% of previous year NSC use (RMSE = 8.6, all other model RMSE > 18.0). By contrast, tree ring $\Delta^{14}C$ at the Utah site was best explained by the model whereby tree growth was entirely supported by current year NSC (RMSE = 17.7, all other model RMSE > 179.0). As a visualization of these model results, assessment of the differences between the mean atmospheric $\Delta^{14}C$ for different modeled proportions and the mean α-cellulose $\Delta^{14}C$ values for each tree site, and their associated SD, is presented in Fig. 4. While we cannot falsify the hypothesis that some small amounts of NSCs were drawn from stores produced earlier than 1 yr before the current growing season, we can conclude that carbon more than 1 yr old is not required to explain the observed $\Delta^{14}C$ time series in Arizona, and no use of stored carbon is needed to explain the Utah $\Delta^{14}C$ data.

Earlywood $\delta^{13}C$ vs VPD for Arizona pine and ponderosa pine

To further test our hypotheses, we quantified relationships between α-cellulose $\delta^{13}C$ and VPD across various temporal aggregations (Fig. 5). In the Arizona trees, the maximum correlation coefficients from regressions of the EW α-cellulose $\delta^{13}C$ time series against running averages of VPD gradually increased from the 1-month average (Fig. 5a; r = 0.64, May) to the 9-month average (Fig. 5a; r = 0.87, previous November–current July). In other words, the correlations gained more power when values from the previous autumn and winter months were combined with values from the current growing season to form means of multiple months. In the Utah trees, the largest correlation coefficients occurred during the EW current growing season and were smaller when the previous autumn and winter months were included. Furthermore, the Utah maximum correlation coefficient values were lower overall, compared to the Arizona values. In Utah, the running maximum correlation coefficients slightly decreased from the 1-month mean VPD (Fig. 5b; r = 0.63, P < 0.0001, June) to the 12-month VPD mean (Fig. 5b; r = 0.56, P < 0.0001, previous November–October).

However, the Arizona pine α-cellulose $\delta^{13}C$ and Arizona VPD time series both exhibit strong upward trends between 1966 and 2014 (Fig. S6), and correlations between time series with a common trend can result in spurious significant correlations. Therefore, we provide a side-by-side comparison of the original data from both sites, as shown in Fig. 5 and with the trends removed (Notes S8; Figs S6, S7). The correlations are less significant after detrending, but the pattern and maxima remain similar.

Results of identical running correlation regression analyses using the SPEI (see Vicente-Serrano *et al*., 2010) and the same α-cellulose $\delta^{13}C$ time series are also available (Notes S9; Fig. S8). The correlation patterns noted in the running correlations from the SPEI analyses for both sites were very similar to those produced using VPD.

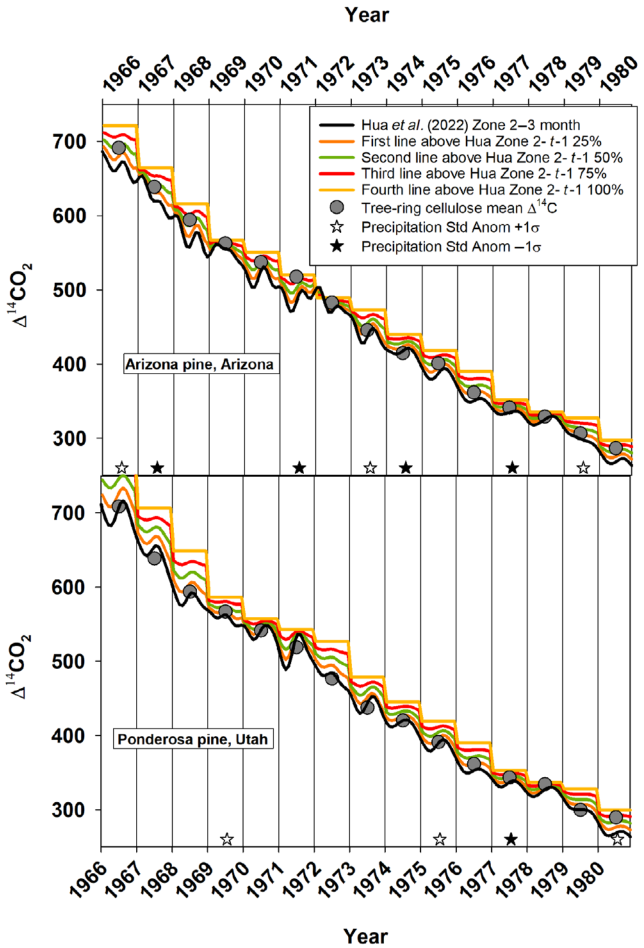

Fig. 3 Modeled $\Delta^{14}C$ cellulose time series predicted from the 3-month means of the current growing season combined in different proportions with the means of April 16 to September 15 for the previous year (e.g. current/previous = 100%/0% (Hua *et al.*, 2022, black), 75%/25% (first line above Hua *et al.*, 2022), 50%/50% (second line above Hua *et al.*, 2022), 25%/75% (third line above Hua *et al.*, 2022), 0%/100% (fourth line above Hua *et al.*, 2022)). Circles are the mean observed values for each year that was measured. Standardized anomalies of precipitation exceeding $\pm1\sigma$ for the mean of the previous November through the current June are indicated for the years 1966–1980 by white and black stars as described in the main text.

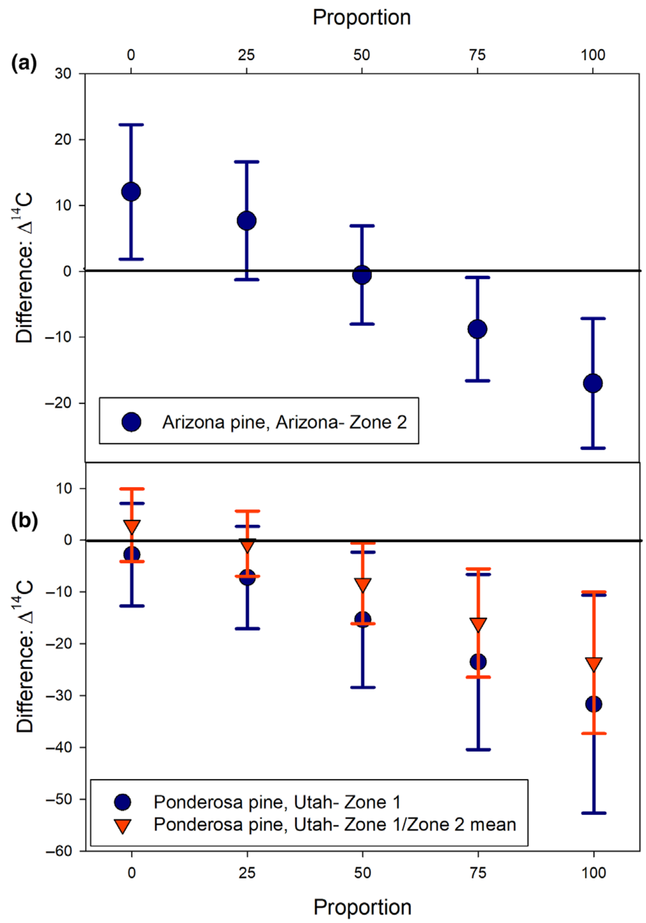

Fig. 4 Differences between the mean modeled $\Delta^{14}C$ values produced using values from the current spring and varying proportions of carbon from the previous growing season based on Zonal $\Delta^{14}C$ values (Hua *et al.*, 2022) compared with the mean α-cellulose $\Delta^{14}C$ values from the tree sites, as shown in Fig. 3, with associated 1σ ranges. (a) Arizona pine modeling (n = 15, df = 13) using Zone 2 values. (b) Ponderosa pine modeling (n = 15, df = 13) using Zone 1 values (circle) and using the mean of Zone 1 and Zone 2 values (triangle). Error bars represent SD.

Discussion

The last in, first out hypothesis for NSC usage

For the past three decades, there has been considerable interest in the role NSC storage pools have in supporting tree growth, especially during annually recurring phenological transitions, episodic droughts, or catastrophic losses of tissue to herbivory or storm damage (Kozlowski, 1992; Sala *et al.*, 2012; Dietze *et al.*, 2014; Hartmann & Trumbore, 2016; Martínez-Vilalta *et al.*, 2016). When phenological needs or environmental stressors cause a critical process within a woody plant to require more NSCs than are immediately available from current season photosynthesis, then either stored NSCs will be mobilized (e.g. Hoch *et al.*, 2003; Kuptz *et al.*, 2011; Richardson *et al.*, 2013; Dobbelstein *et al.*, 2018; Furze *et al.*, 2018), or the critical process will be downregulated (e.g. de Dios & Gessler, 2021; Huang *et al.*, 2021). As early as Kozlowski's comprehensive 1992 review on carbohydrates in plants, it was recognized that while some stores are deposited and remobilized at timescales of days to months, others can remain inert for years to decades. One of the principal questions that has captured the interest of forest ecologists since that review is: Do plants access the older stored carbon pools, and if so, under what conditions?

Use of the ^{14}C content of tissues produced during the nuclear-testing bomb spike has provided insight into that question. ^{14}C studies conducted to date have shown that in foliar, root, and stemwood tissues, NSC stores are indeed used for production, but those stores are commonly not older than 1–2 yr (Gaudinski *et al.*, 2001; Richardson *et al.*, 2015). In a study of the radial distribution of the age of NSC stores in red oak and

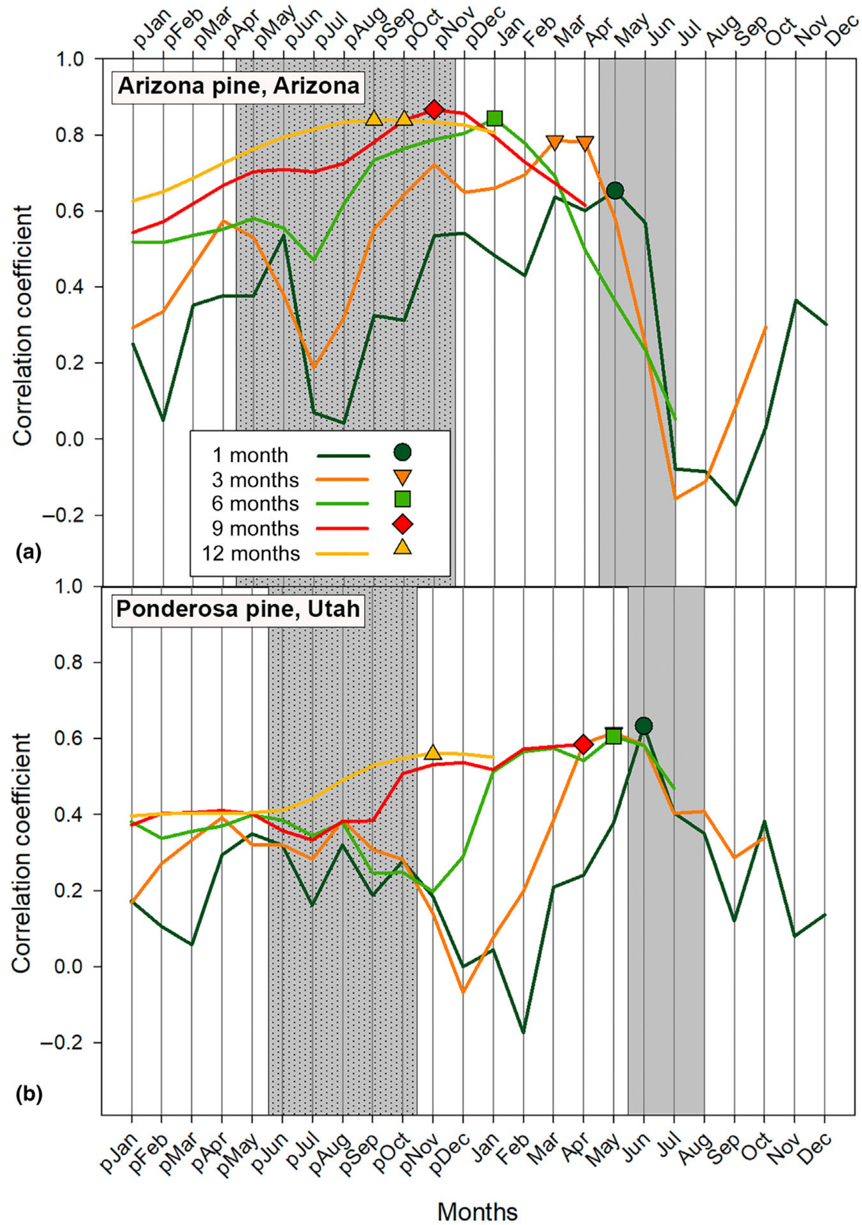

Fig. 5 Running averages of $\delta^{13}C$ in EW α-cellulose regressed against VPD in (a) Arizona pine, and (b) ponderosa pine, Utah. The correlation coefficients are plotted on the first month of the multi-month average, while the colored lines indicate various temporal aggregations. The symbols are plotted at the position of the maximum observed correlation for each multi-month averaging scheme (e.g. previous November–July was plotted on November). The approximate timing of the previous growing season (beginning of cell enlargement to the end of cell maturation) and the current growing season that produces the EW tree ring fraction (beginning of cell enlargement to the end of cell maturation) is shown by the stippled gray shading and the solid gray shading, respectively.

white pine, Richardson *et al.* (2015) showed that the most recent 5 yr of stemwood (i.e. the five outermost growth rings) included NSC stores in parenchyma rays that were < 1 yr old. Older NSC pools were present in the stemwood, but only in wood > 5 yr old, perhaps reflecting the past preferential use of younger NSC pools during wood production and radial mixing of older with newer pools. These studies support a pattern of NSC formation and use that is best described as 'last in, first out'. Following this pattern, the construction of woody tissues would rely on the preferential use of a young pool of photosynthate and stored NSCs, while leaving older NSC pools unconsumed. The inevitable outcome of 'last in, first out' NSC usage supported a two-pool model – one of fast cycling, younger NSCs and one of slower cycling, older NSCs – that was originally proposed by Richardson *et al.* (2013).

In more recent work, Peltier *et al.* (2023) showed that during multiple consecutive drought years, the mean age of stemwood NSC pools in pinyon pine trees decreased. This was attributed to long-term reductions in photosynthetic production that shifted the use of carbon sources toward stored NSC pools. These results are consistent with the 'last in, first out' hypothesis, but they clarify that during conditions of decreased carbon acquisition, older NSC pools are accessible. It is worth noting that we did not find any broad shift in the age of carbon utilized for growth during (or following) wet and dry anomalies. The Peltier *et al.* (2023) study provides a hypothesis to explain this dynamic, whereby older carbon reserves may be only utilized following long-term (i.e. decadal scale) drought, which was not apparent at either of our sites during the years studied. The use of older carbon has also been found following other extreme stressors such as stem girdling, defoliation, and widespread root mortality (Vargas *et al.*, 2009; Muhr *et al.*, 2018; D'Andrea *et al.*, 2019), though most of these studies have focused on angiosperm species.

We acknowledge that the two-pool model used here is likely a simplification. Despite the prominence of the 'last in, first out' model, there could be a much wider mix of NSC ages used to support radial growth, with the age distribution of carbon tailing off significantly after a few years (Herrera-Ramírez *et al.*, 2020). However, we do highlight that any use of older carbon would substantially decrease the proportional contribution of previously assimilated carbon at the Arizona site and thus strengthen our findings regarding the prevalent use of newly assimilated carbon.

Validity of using the bomb spike radiocarbon time series to predict cellulose age

Comparisons between time series of atmospheric $\Delta^{14}CO_2$ and $\Delta^{14}C$ values from the dried tissues of winter/spring annuals collected in southeastern Arizona and northeastern Utah indicate similar values for most data points (Fig. 1). We observed that the $\Delta^{14}C$ values from cellulose in Utah annuals matched Zone 1 better than Zone 2 for values between 1966 and 1973. After 1973, however, the zonal estimates for atmospheric $\Delta^{14}C$ for the two zones converge, and the Utah annuals match the converged zonal pattern even more precisely than the Arizona annuals. The close and consistent match between $\Delta^{14}C$ values from annuals at the two sites with their respective atmospheric $\Delta^{14}CO_2$ zones provided independent validation for our starting assumption that the $\Delta^{14}C$ values from EW cellulose should align well with each respective atmospheric time series if the only carbon used was assimilated during the same year as ring formation.

Testing the hypotheses concerning the use of older carbon stores in tree rings

With this study we sought to test three hypotheses: (1) that a significant amount of 'old', slow-cycling carbon, defined here as carbon assimilated in distant (> 2 yr) prior years, is present in the EW of annual rings; (2) that a significant amount of 'new', fast-cycling carbon assimilated in recent years ($\leq$ 2 yr) was used to produce the EW of annual rings; and (3) that only carbon from the current growing season was used to produce the EW of annual rings. Our radiocarbon observations were conducted across a 15-yr time series from multiple trees at two different sites, analyzed separately, and included a broad range of climate conditions, with both wetter and drier climate anomalies. Based solely on comparisons between $\Delta^{14}C$ values from Arizona pine EW cellulose and Zone 2 atmospheric $\Delta^{14}CO_2$ values (Fig. 2), there is no evidence for the use of 'old', slow-cycling stored carbon, so the first hypothesis is not supported. There is some evidence for the use of 'recent', fast-cycling stored carbon, supporting the second hypothesis, but not the third hypothesis, wherein only 'new' carbon from the current growing season was used. Comparisons of observed and predicted cellulose $\Delta^{14}C$ values, generated from mean atmospheric $\Delta^{14}CO_2$ using different proportions of input from the previous growing season (0, 25, 50, 75, 100%), support the idea that the offsets between cellulose $\Delta^{14}C$ and atmospheric $\Delta^{14}C$ can be completely explained using a combination of current photosynthate and photosynthate produced during the previous year (Fig. 3) Comparison of the differences between the modeled proportions and the mean cellulose $\Delta^{14}C$ for each year indicates that, on average, 50% of the carbon used during each growing season at the Arizona site may have come from photoassimilation during the previous growing season (Fig. 4a).

Most observed $\Delta^{14}C$ values from the Utah ponderosa pine EW α-cellulose closely matched values from the Zone 1 atmospheric $\Delta^{14}CO_2$ time series (Fig. 3). Almost entirely, the observed $\Delta^{14}C$ α-cellulose values fell below the modeled values that would indicate incorporation of significant amounts of carbon assimilated during previous growing seasons. Comparison of the differences between the modeled proportions using the Zone 1 values and the mean cellulose $\Delta^{14}C$ for each year indicates that, on average, no carbon was used from the previous growing season (0%, Fig. 4b), supporting the third hypothesis wherein no carbon from previous growing seasons was used to produce the cellulose.

Yet we recognize that the Northeastern Utah tree site falls close to the geographic boundary between the Zone 1 and Zone 2 time series, as distinguished by Hua *et al.* (2013, 2022). It is possible that the complications of being situated at the transition between two zones influenced our results. Using the average of the Zone 1 and Zone 2 values as input for modeling the proportions results in a reduced minimum difference and reduced minimum 1σ value as compared with Zone 1 modeling (Fig. 4b), with the reduced values occurring when 25% of the carbon incorporated came from the previous growing season, a finding that supports the second hypothesis. In both models, the 1σ range of the minimum difference overlaps the ranges of the 1σ ranges for the other proportions, so interannual changes in the proportion of carbon incorporated from the previous growing season are possible. However, even accepting the possibility of some uncertainty in the source of $^{14}CO_2$ at the Utah site, there remains no evidence for the use of stored carbon from a slow-cycling pool older than 1 yr. This is not to say that the use of older carbon is impossible at this site; rather, that its use is not necessary to explain the observed trends in $\Delta^{14}C$.

α-cellulose $\delta^{13}C$ time series and stored carbon

As a second test of our hypotheses, we also sought to detect which carbon was used to support radial growth using α-cellulose $\delta^{13}C$ time series by linking $\delta^{13}C$ to VPD anomalies at various temporal scales. In Arizona pine, we observed significant correlations between cellulose $\delta^{13}C$ and monthly VPD, with May providing the highest correlation. The maximum correlations increased consistently and shifted back in time when additional months were included to a maximum correlation against the previous November through July (Fig. 5a). From this result, we concluded that the trees partially incorporated photosynthate formed during the previous winter. This finding is consistent with the fact that this species occurs in a relatively mild winter and spring climate, providing a potential capacity for overwinter photosynthesis. It is also worth noting that the longer SPEI aggregations showed larger correlation coefficients with the previous year's climate than the shorter SPEI aggregations, supporting our $\Delta^{14}CO_2$ findings that both new and 1-yr-old carbon were likely used to support radial growth at this site.

Conversely, correlation coefficients from regressions of the Utah pine (Fig. 5b) showed reliance on photosynthate formed only during the current growing season, consistent with the harsher winter climate and complete winter dormancy. We also note that correlation coefficients for this population were lower than for the Arizona site, indicating a lower climate sensitivity generally.

In sum, the $\delta^{13}C$ data indicate reliance on stored carbon from the fall, winter, and pre-growing season spring in the Arizona pines, while the $\delta^{13}C$ values from the Utah pines provide no evidence for the incorporation of photosynthate formed before the current growing season. Other studies attempting moving window correlation analyses on tree-ring $\delta^{13}C$ are rare, and rarer still for the EW of arid conifers. However, previous work that has attempted to isolate the key climatic windows controlling $\delta^{13}C$ variability has reached similar conclusions: that current year spring aridity and previous fall/winter aridity are key determinants (McCarroll *et al.*, 2017; Maxwell *et al.*, 2020; Fan *et al.*, 2021). Our analysis here provides a critical secondary source of evidence that the carbon used by our pine populations was quite young.

The case for the use of overwinter NSC stores in Arizona pine

Richardson *et al.* (2013) and Furze *et al.* (2018) reported marked seasonal dynamics in the stemwood NSC pools in three deciduous and two evergreen species in the northeastern United States. During the winter, there was a clear mobilization of starch, which had been stored during the previous growing season, to form sugars in all species. The free sugars remained at high concentrations until spring, when growth demands increased. In this type of seasonal pattern, we would expect the $\delta^{13}C$ ratios of newly produced EW to correlate with the climate of the previous summer, when the NSC stores were originally formed. This was not the pattern of correlation we observed for Arizona pine trees.

We interpret our observations with Arizona pine as lending support for the springtime use of NSC stores produced during the prior winter of the same year. Overwinter photosynthesis has long been recognized in evergreen conifers (e.g. Pallardy, 2008), and in the Santa Catalina Mountains of southeastern Arizona has been specifically reported for *P. arizonica* (e.g. Potts *et al.*, 2017) and *P. ponderosa* (Fritts, 1976; Potts *et al.*, 2017). Given the lack of active tree growth during winter months, it is likely that much of the winter-produced photosynthate was stored and is available for growth during the following growing season.

Conclusions

There is still considerable work to be done to resolve the locations and ages of NSC stores of different ages in trees, the degree to which stored pools mix with one another, and the degree to which those stores are available to support tree growth. Regarding the first half of the EW tissues of semiarid, montane pines, our results indicate that: (1) nearly all of the photosynthate that is incorporated into biomass was assimilated during the current growing season for Utah *P. ponderosa*, (2) photosynthate from both the current growing season and the previous year (likely in winter) was utilized by Arizona *P. arizonica*. While we cannot refute the possibility that carbon > 1 yr old was used to support the growth of *P. arizonica*, this amount would need to be extremely small in order to explain the observed $\Delta^{14}C$ values in this species.

The evidence for incorporation of carbon from several months before the current growing season in the EW growth of Arizona pine necessitates a caveat regarding the use of subannual tree-ring cellulose for climate reconstruction. This is especially relevant given the increasingly frequent efforts to partition the stable isotope dynamics of annual tree rings into seasonal subdivisions (Szejner *et al.*, 2016; Belmecheri *et al.*, 2018; Monson *et al.*, 2018). The effect of any current season climate on current season stable carbon isotope values may be diluted by the incorporation of carbon from the previous winter and/or the previous growing season. This influence may not be systematic, so removal of the effect during the post-processing of stable isotope observations may not be possible.

The frequent use of some older carbon may be related to physiological differences between trees that experience only partial winter dormancy and those that experience complete winter dormancy, because evidence for the incorporation of stored carbon was almost entirely lacking in the ponderosa pine from northeastern Utah, where temperatures currently ensure complete winter dormancy. Note that this distinction is not likely to be constant through time. Increasing temperatures at higher latitudes may soon allow photosynthesis during the winter in locations where such activity was previously temperature-limited. And by extension, increasing winter temperatures in locations such as the mountains of southern Arizona may increase maintenance respiration demands during the winter, with consequent reductions in the availability of stored carbon during the subsequent growing season. Future studies targeting older trees, stands that vary in winter dormancy, and years with notable climate anomalies (i.e. when the use of stored carbon may be more prevalent) are necessary to generate a mechanistic understanding of old carbon use.

Acknowledgements

This study was supported by the Macrosystems program in the Emerging Frontiers section of the U.S. National Science Foundation (NSF award 1065790) and the Ecosystems Program in the Division of Environmental Biology (NSF Award 1754430). SAK was supported by the U.S. National Science Foundation Division of Environmental Biology Grant 2331162 and U.S. National Science Foundation Dynamics of Integrated Socio-Environmental Systems award 2408954. We appreciate the assistance provided by George Ferguson of the University of Arizona Herbarium and Mitchell Power and Allison Isaksonis of the Garrett Herbarium at the University of Utah in obtaining annual specimens, and Soumaya Belmecheri and Brandon Strange for their help with some of the data analysis.

Competing interests

None declared.

Author contributions

WEW, JRE and RKM planned and designed the research. WEW and SAK conducted fieldwork and analyzed data. WEW, SAK and RKM wrote the manuscript. SAK and WEW contributed equally to this work.

ORCID

James R. Ehleringer https://orcid.org/0000-0003-2050-3636
Steven A. Kannenberg https://orcid.org/0000-0002-4097-9140
Russell K. Monson https://orcid.org/0000-0002-7671-4371
William E. Wright https://orcid.org/0000-0003-1359-2327

Data availability

Radiocarbon data produced as part of this study are available in Table S1. All other data are publicly available via the sources described in the Materials and Methods section.

References

Belmecheri S, Wright WE, Szejner P, Morino KA, Monson R. 2018. Carbon and oxygen isotope fractionations in tree rings reveal interactions between cambial phenology and seasonal climate. *Plant, Cell & Environment* **41**: 2758–2772.

Beverly RK, Beaumont W, Tauz D, Ormsby KM, von Reden KF, Santos GM, Southon JR. 2010. The keck carbon cycle AMS Laboratory, University of California, Irvine: status report. *Radiocarbon* **52**: 301–309.

Carbone MS, Czimczik CI, Keenan TF, Murakami PF, Pederson N, Schaberg PG, Xu X, Richardson AD. 2013. Age, allocation and availability of nonstructural carbon in mature red maple trees. *New Phytologist* **200**: 1145–1155.

Daly C, Halbleib M, Smith JI, Gibson WP, Doggett MK, Taylor GH, Curtis J, Pasteris PP. 2008. Physiographically sensitive mapping of climatological temperature and precipitation across the conterminous United States. *International Journal of Climatology* **28**: 2031–2064.

D'Andrea E, Rezaie N, Battistelli A, Gavrichkova O, Kuhlmann I, Matteucci G, Moscatello S, Proietti S, Scartazza A, Trumbore S *et al.* 2019. Winter's bite: beech trees survive complete defoliation due to spring late-frost damage by mobilizing old C reserves. *New Phytologist* **224**: 625–631.

De Dios VR, Gessler A. 2021. Sink and source co-limitation in the response of stored non-structural carbohydrates to an intense but short drought. *Trees* **35**: 1751–1753.

Dietze MC, Sala A, Carbone MS, Czimzik CI, Mantooth JA, Richardson AD, Vargas R. 2014. Nonstructural carbon in woody plants. *Annual Review of Plant Biology* **65**: 667–687.

Dobbelstein E, Fink D, Öner-Sieben S, Czempik L, Lohaus G. 2018. Seasonal changes of sucrose transporter expression and sugar partitioning in common European tree species. *Tree Physiology* **39**: 284–299.

Fan Y, Shang H, Yu S, Wu Y, Li Q. 2021. Understanding the representativeness of tree rings and their carbon isotopes in characterizing the climate signal of Tajikistan. *Forests* **12**: 1215.

Ficklin DL, Novick KA. 2017. Historic and projected changes in vapor pressure deficit suggest a continental-scale drying of the United States atmosphere. *Journal of Geophysical Research: Atmospheres* **122**: 2061–2079.

Fiorella RP, Kannenberg SA, Anderegg WRL, Monson RK, Ehleringer JR. 2022. Heterogeneous isotope effects decouple conifer leaf and branch sugar $\delta^{18}O$ and $\delta^{13}C$. *Oecologia* **198**: 357–370.

Fritts HC. 1976. *Tree rings and climate.* New York, NY: Elsevier.

Fu P-L, Griessinger J, Gebrekirstos A, Fan Z-X, Bräuning A. 2017. Earlywood and latewood stable carbon and oxygen isotope variations in two pine species in southwestern China during the recent decades. *Frontiers in Plant Science* **7**: 2050.

Furze ME, Hartmann H, Trumbore S. 2018. Detours on the phloem sugar highway: stem carbon storage and remobilization. *Current Opinion in Plant Biology* **43**: 89–95.

Gaudinski J, Trumbore S, Davidson E, Cook A, Markewitz D, Richter D. 2001. The age of fine-root carbon in three forests of the eastern United States measured by radiocarbon. *Oecologia* **129**(3): 420–429.

Gessler A, Brandes E, Keitel C, Boda S, Kayler ZE, Granier A, Barbour M, Farquhar GD, Treydte K. 2013. The oxygen isotope enrichment of leaf-exported assimilates – does it always reflect lamina leaf water enrichment? *New Phytologist* **200**: 144–157.

Hartmann H, Trumbore S. 2016. Tansley review–understanding the roles of nonstructural carbohydrates in forest trees–from what we can measure to what we want to know. *New Phytologist* **211**: 386–403.

Herrera-Ramírez D, Muhr J, Hartmann H, Römermann C, Trumbore S, Sierra CA. 2020. Probability distributions of nonstructural carbon ages and transit times provide insights into carbon allocation dynamics of mature trees. *New Phytologist* **226**: 1299–1311.

Hoch G, Richter A, Körner C. 2003. Non-structural carbon compounds in temperate forest trees. *Plant, Cell & Environment* **26**: 1067–1081.

Hua Q, Barbetti M, Rakowski AZ. 2013. Atmospheric radiocarbon for the period 1950–2010. *Radiocarbon* **55**: 2059–2072.

Hua Q, Turnbull JC, Santos GM, Rakowski AZ, Ancapichún S, De Pol-Holz R, Hammer S, Lehmann SJ, Levin I, Miller JB *et al.* 2022. Atmospheric radiocarbon for the period 1950–2019. *Radiocarbon* **64**: 724–745.

Huang J, Hammerbacher A, Gershenzon J, van Dam NM, Sala A, McDowell NG, Chowdury S, Gleixner G, Trumbore A, Hartmann H. 2021. Storage of carbon reserves in spruce trees is prioritized over growth in the face of carbon limitation. *Proceedings of the National Academy of Sciences, USA* **18**: 118.

Kagawa A, Sugimoto A, Maximov TC. 2006a. $^{13}CO2$ pulse-labelling of carbon reveals carbon allocation within and between tree rings. *Plant, Cell & Environment* **29**: 1571–1584.

Kagawa A, Sugimoto A, Maximov TC. 2006b. Seasonal course of translocation, storage and remobilization of ^{13}C pulse-labeled photoassimilate in naturally growing *Larix gmelinii* saplings. *New Phytologist* **171**: 793–804.

Kimak A, Leuenberger M. 2015. Are carbohydrate storage strategies of trees traceable by early–latewood carbon isotope differences? *Trees* **29**: 859–870.

Kozlowski TT. 1992. Carbohydrate sources and sinks in woody plants. *The Botanical Review* **58**: 107–222.

Krepkowski J, Gebrekirstos A, Shibistova O, Bräuning A. 2013. Stable carbon isotope labeling reveals different carry-over effects between functional types of tropical trees in an Ethiopian mountain forest. *New Phytologist* **199**: 431–440.

Kuptz D, Fleischmann F, Matyssek R, Grams TEE. 2011. Seasonal pattern of carbon allocation to respiratory pools in 60-year-old deciduous (*Fagus sylvatica*) and evergreen (*Picea abies*) trees assessed via whole-tree stable carbon isotope labelling. *New Phytologist* **191**: 160–172.

Leavitt SW, Roden J. 2022. Chapter 1 isotope dendrochronology: historical perspective. In: Siegwolf RTW, Brooks JR, Roden J, Saurer M, eds. *Stable isotopes in tree rings. Tree physiology, vol. 8.* Cham, Switzerland: Springer, 3–20.

Martínez-Vilalta J, Sala A, Asensio D, Galiano L, Hoch G, Palacio S, Piper FI, Lloret F. 2016. Dynamics of non-structural carbohydrates in terrestrial plants: a global synthesis. *Ecological Monographs* **86**: 495–516.

Maxwell SR, Belmecheri S, Taylor AH, Davis KJ, Ocheltree TW. 2020. Carbon isotope ratios in tree rings respond differently to climatic variations than tree-ring width in a mesic temperate forest. *Agricultural and Forest Meteorology* **288**: 108014.

McCarroll D, Gagen MH, Loader NJ, Robertson I, Anchukaitis KJ, Los S, Young G, Jalkanen R, Kirchhefer A, Waterhouse JS. 2008. Correction of tree ring stable carbon isotope chronologies for changes in the carbon dioxide content of the atmosphere. *Geochimica et Cosmochimica Acta* **73**: 1539–1547.

McCarroll D, Whitney M, Young G, Loader N, Gagen M. 2017. A simple stable carbon isotope method for investigating changes in the use of recent versus old carbon in oak. *Tree Physiology* **37**: 1021–1027.

Mildner M, Bader MK-F, Baumann C, Körner C. 2015. Respiratory fluxes and fine root responses in mature *Picea abies* trees exposed to elevated atmospheric CO_2 concentrations. *Biogeochemistry* **124**(1–3): 95–111.

Monson RK, Szejner P, Belmecheri S, Morino K, Wright WE. 2018. Finding the seasons in tree ring stable isotope ratios. *American Journal of Botany* **105**: 819–821.

Morino K, Minor RL, Barron-Gafford GA, Brown PM, Hughes MK. 2021. Bimodal cambial activity and false-ring formation in conifers under a monsoon climate. *Tree Physiology* **41**(10): 1893–1905.

Muhr J, Trumbore S, Higuchi N, Kunert N. 2018. Living on borrowed time – Amazonian trees use decade-old storage carbon to survive for months after complete stem girdling. *New Phytologist* **220**: 111–120.

Novick KA, Ficklin DL, Stoy PC, Williams CA, Bohrer G, Oishi AC, Papuga SA, Blanken PD, Noormets A, Sulman BN *et al.* 2016. The increasing importance of atmospheric demand for ecosystem water and carbon fluxes. *Nature Climate Change* **6**: 1–5.

Pallardy SG. 2008. Chapter 5. Photosynthesis. In: *Physiology of woody plants, 3rd edn*. San Diego, CA: Academic Press, 454.

Peltier DMP, Carbone MS, McIntire CD, Robertson NR, Thompson RA, Malone S, Friedman M, LeMoine J, Richardson AD, McDowell NG *et al.* 2023. Carbon starvation following a decade of experimental drought exhausts old reserves in *Pinus edulis*. *New Phytologist* **20**: 19119.

Potts DL, Minor RL, Braun Z, Barron-Gafford GA. 2017. Photosynthetic phenological variation may promote coexistence among co-dominant tree species in a Madrean sky Island mixed conifer forest. *Tree Physiology* **37**: 1229–1238.

Richardson AD, Carbone MS, Huggett BA, Furze ME, Czimczik CI, Walker JC, Xu X, Schaberg PG, Murakami P. 2015. Distribution and mixing of old and new nonstructural carbon in two temperate trees. *New Phytologist* **206**: 590–597.

Richardson AD, Carbone MS, Keenan TF, Czimczik CI, Hollinger DY, Murakami P, Schaberg PG, Xu X. 2013. Seasonal dynamics and age of stemwood nonstructural carbohydrates in temperate forest trees. *New Phytologist* **197**: 850–861.

Rinne-Garmston KT, Tang Y, Sahlstedt E, Adamczyk B, Saurer M, Salmon Y, Carrasco MDRD, Hölttä T, Lehmann MM, Mo L *et al.* 2023. Drivers of intra-seasonal δ^{13} C signal in tree-rings of *Pinus sylvestris* as indicated by compound-specific and laser ablation isotope analysis. *Plant, Cell & Environment* **46**: 2649–2666.

Sala A, Woodruff DR, Meinzer FC. 2012. Carbon dynamics in trees: feast or famine? *Tree Physiology* **32**: 764–775.

Sheppard P, Comrie A, Packin G, Angersbach K, Hughes M. 2002. The climate of the US Southwest. *Climate Research* **21**: 219–238.

Suess SE. 1955. Radiocarbon concentration in modern wood. *Science* **122**: 415–417.

Switsur VR, Waterhouse JS, Field EM, Carter AHC, Loader NJ. 1995. Stable isotope studies in tree rings from oak—techniques and some preliminary results. *Paläoklimaforschung* **15**: 129–140.

Szejner P, Wright WE, Babst F, Belmecheri S, Trouet V, Leavitt SW, Ehleringer JR, Monson RK. 2016. Latitudinal gradients in tree ring stable carbon and oxygen isotopes reveal differential climate influences of the North American Monsoon System. *Journal of Geophysical Research: Biogeosciences* **121**: 1978–1991.

Vargas R, Trumbore SE, Allen MF. 2009. Evidence of old carbon used to grow new fine roots in a tropical forest. *New Phytologist* **182**: 710–718.

Vicente-Serrano SM, Beguería S, López-Moreno JI. 2010. A multiscalar drought index sensitive to global warming: the standardized precipitation evapotranspiration index. *Journal of Climate* **23**: 1696–1718.

Willyard A, Gernandt DS, Potter K, Hipkins V, Marquardt P, Mahalovich MF, Langer SK, Telewski FW, Cooper B, Douglas C *et al.* 2016. Pinus ponderosa: a checkered past obscured four species. *American Journal of Botany* **104**: 161–181.

Yuan W, Zheng Y, Piao S, Ciais P, Lombardozzi D, Wang Y, Ryu Y, Chen G, Dong W, Hu Z *et al.* 2019. Increased atmospheric vapor pressure deficit reduces global vegetation growth. *Science Advances* **5**: eaax1396.

Supporting Information

Additional Supporting Information may be found online in the Supporting Information section at the end of the article.

Fig. S1 Representative *Pinus arizonica* tree core and EW subdivisions.

Fig. S2 Representative *Pinus ponderosa* tree core and EW subdivisions.

Fig. S3 Time series of standardized climate anomalies for the Arizona site.

Fig. S4 Time series of standardized climate anomalies for the Utah site.

Fig. S5 Time series of the last day of continuous snowpack in Utah.

Fig. S6 Plot of EW cellulose δ^{13}C and VPD data to show the positive trends.

Fig. S7 Figure showing that the use of detrended VPD data does not change the results.

Fig. S8 Figure showing that the use of SPEI data does not change the results.

Methods S1 Additional description of tree-ring processing and isotope sample preparation.

Notes S1 Description of the ponderosa pine complex.

Notes S2 Description of general dendrochronological features at each site.

Notes S3 Additional information regarding annual plant sampling and sourcing.

Notes S4 Justification for combining two δ^{13}C time series from the Arizona site.

Notes S5 Information on error in Δ^{14}C and δ^{13}C data.

Notes S6 Discussion on the use of standardized climate anomalies.

Notes S7 Explaining an anomalous Utah $\Delta^{14}C$ value with Snotel data.

Notes S8 Discussion about detrending VPD trends.

Notes S9 Discussion on the use of SPEI instead of VPD.

Table S1 Tree-ring and annual radiocarbon data.

Please note: Wiley is not responsible for the content or functionality of any Supporting Information supplied by the authors. Any queries (other than missing material) should be directed to the *New Phytologist* Central Office.